J. Fluid Mech. (1978), *vol.* 86, *part* 1, *pp.* 49–65
Printed in Great Britain

The heat/mass transfer to a finite strip at small Péclet numbers

By R. C. ACKERBERG, R. D. PATEL AND S. K. GUPTA

Department of Chemical Engineering, Polytechnic Institute of New York, Brooklyn

(Received 8 August 1977)

The problem of heat transfer (or mass transfer at low transfer rates) to a strip of finite length in a uniform shear flow is considered. For small values of the Péclet number (based on wall shear rate and strip length), diffusion in the flow direction cannot be neglected as in the classical Leveque solution. The mathematical problem is solved by the method of matched asymptotic expansions and expressions for the local and overall dimensionless heat-transfer rate from the strip are found. Experimental data on wall mass-transfer rates in a tube at small Péclet numbers have been obtained by the well-known limiting-current method using potassium ferrocyanide and potassium ferricyanide in sodium hydroxide solution. The Schmidt number is large, so that a uniform shear flow can be assumed near the wall. Experimental results are compared with our theoretical predictions and the work of others, and the agreement is found to be excellent.

1. Introduction

Measurement of the heat transfer from an isothermal strip placed on an otherwise insulated wall in a uniform shear flow has been a useful indirect technique for estimating the velocity gradient at the wall. This method is based on the well-known thermal boundary-layer solution of Leveque (1928), which is valid when the Péclet number Pe is large and axial diffusion is negligible. Recently it has been found desirable to consider heat transfer from extremely small elements, such as the probes used in monitoring blood flow in arteries. In these cases the strip is so narrow that axial diffusion cannot be ignored, and in fact, the heat transfer is completely dominated by edge effects. It is this problem that is considered in this paper. The analogous mass-transfer problem, at low mass-transfer rates, is identical to the heat-transfer problem and our work can also be applied to this case.

The first attempt to account for the leading- and trailing-edge effects for a small strip, where axial diffusion is important, is due to Ling (1963), who considered a steady shear flow with a linear velocity profile. Ling divided the transfer surface into three regions: (1) a leading-edge zone where axial diffusion must be included, (2) a central zone where axial diffusion is negligible and the Leveque solution is valid and (3) a trailing-edge zone where axial diffusion is again important. Ling obtained the solutions in zones 1 and 3 using numerical integration and found that if $Pe > 5000$ the entire surface could be assumed to be in zone 2 for the purpose of calculating the overall heat transfer from the surface, i.e. the edges had a negligible effect.

Springer & Pedley (1973) and Springer (1974) considered the leading- and trailing-

edge regions of a semi-infinite flat plate separately in an effort to isolate the edge effects. In both cases the Leveque solution was assumed either downstream of the leading edge or upstream of the trailing edge and the Wiener–Hopf technique was used to obtain analytical solutions. By integrating the heat flux over a section of the thermal wake, Springer obtained an estimate of the variation of the Nusselt number Nu with $Pe^{\frac{1}{2}}$. In addition he found that for the boundary-layer solution to be valid anywhere on the plate it was necessary to have $Pe > 22$. Popov (1975) considered the same problem as Springer & Pedley (1973) for the heat transfer from a leading edge, and obtained similar results.

Newman (1973), apparently unaware of Ling's work, also carried out numerical integrations in the leading- and trailing-edge regions. The numerical results he obtained for the coefficients of the square-root singularities in the local flux at the leading and trailing edges can be compared directly with Springer & Pedley's coefficient for the leading edge and Springer's coefficient for the trailing edge, which he tabulated *vs.* $Pe^{\frac{1}{2}}$.† The leading-edge coefficients agree to two decimal places and the trailing-edge coefficients differ by less than 4 % when $Pe \geqslant 25$, which is about the smallest value for which Springer's results are reliable. Newman (1973) combined his analytical and numerical results to obtain an equation relating Nu and Pe (equation (361) of his paper) with an error term $O(Pe^{-\frac{2}{3}})$.

The mathematical formulation of our problem is given in § 2 and the first-order solutions in the inner and outer expansions are obtained. In § 3 the second-order outer solution is found using a Fourier transform technique, and the asymptotic behaviour of this solution is determined. The matching of the first-order terms leads to a gauge function which is proportional to $(\ln Pe + \text{constant})^{-1}$, but unlike the Stokes flow past a cylinder, convective terms *do* enter the inner expansion. The first three terms and the eigenfunctions of the inner expansion are obtained in § 4, and in § 5 an extensive matching procedure is carried out which helps to determine the third-order solution in the outer expansion. An inconsistency in the matching forces the introduction of an additional term in both the inner and the outer expansion, which changes the heat flux. In § 6 the heat flux from the strip is found; if, however, the heat flux is specified, as for a heated element, the temperature of the strip can be predicted. The temperature distribution far downstream in the wake is determined in § 7.

Since we were unaware of any experimental results for which $Pe < 5$, it was desirable to verify the theoretical predictions experimentally. The experimental apparatus and technique are described in § 8, and experimental data for small Pe are compared with our theoretical results in § 9.

2. Mathematical formulation

We consider steady uniform shear flow past a heated (or cooled) isothermal strip of length L which is embedded in an insulated wall and maintained at a constant temperature T_0 (see figure 1). At large distances from the strip the fluid temperature is fixed at T_∞. Denoting dimensional variables with bars, we introduce the following non-dimensional variables:

$$x = \bar{x}/(\tfrac{1}{2}L), \quad y = \bar{y}/(\tfrac{1}{2}L), \quad T = (\bar{T} - T_0)/(T_\infty - T_0). \tag{2.1}$$

† Some care is required in making this comparison owing to a factor of 2 which appears in Newman's non-dimensionalization and Péclet number.

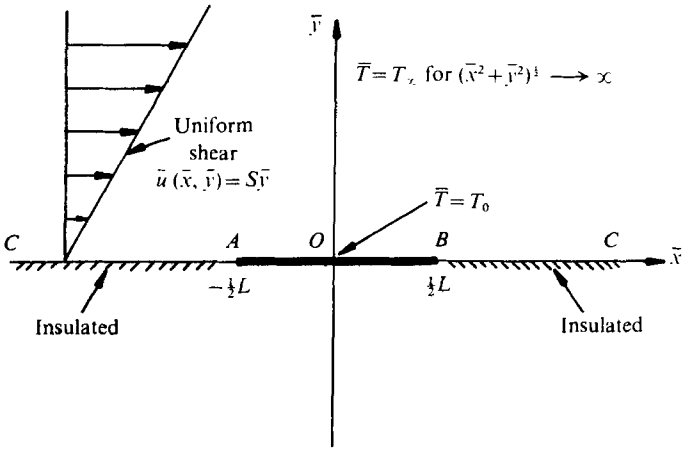

FIGURE 1. Flow geometry.

The governing convection–diffusion equation for a fluid of constant properties may be written as

$$\epsilon y\,\partial T/\partial x = \nabla^2 T \quad (-\infty < x < \infty,\ y \geqslant 0;\ 0 < \epsilon \ll 1), \tag{2.2}$$

where ∇^2 is the Laplacian with respect to (x, y). The small parameter $\epsilon = SL^2/4\kappa$, where κ is the thermal diffusivity, S is the constant shear rate at the wall and the Péclet number, based on the strip length, is given by $Pe = 4\epsilon$. The boundary conditions require

$$T = 0 \quad \text{for} \quad y = 0, \quad |x| < 1, \tag{2.3}$$

$$\partial T/\partial y = 0 \quad \text{for} \quad y = 0, \quad |x| > 1, \tag{2.4}$$

$$T \to 1 \quad \text{for} \quad (x^2+y^2)^{\frac{1}{2}} \to \infty. \tag{2.5}$$

Our objective is to find uniformly valid asymptotic solutions for $\epsilon \to 0$ by the method of matched asymptotic expansions.

First-order inner solution

If we formally put $\epsilon \equiv 0$ in (2.2) and assume

$$T(x, y) \sim g(\epsilon)\, t_0(x, y),$$

where $g(\epsilon)$ is a gauge function to be determined, we obtain

$$\nabla^2 t_0 = 0. \tag{2.6}$$

A solution of (2.6) subject to the boundary conditions (2.3)–(2.5) does not exist. The explanation of this paradox is that when viewed from large distances the strip must appear to be a point sink,† and solutions of Laplace's equation with this characteristic must exhibit a logarithmic divergence for $r = (x^2+y^2)^{\frac{1}{2}} \to \infty$. A solution of (2.6) with this property which satisfies (2.3) and (2.4) and has integrable flux singularities at the edges, i.e.

$$\left| \int_{\mathscr{L}} \left[\frac{\partial T}{\partial y} \right]_{y=0} dx \right| < \infty, \tag{2.7}$$

† In the non-dimensional formulation (2.2)–(2.5), heat is flowing towards the strip from infinity.

where $\mathscr{L}$ is an $O(1)$ length of strip including a *single* end point, is given by

$$t_0(x, y) = \operatorname{Re} \ln [z + (z^2 - 1)^{\frac{1}{2}}], \tag{2.8}$$

where $z = x + iy$ and the function $(z^2 - 1)^{\frac{1}{2}}$ is regular in the z plane, which has been cut along the strip $y = 0$, $|x| < 1$. The principal value of the logarithm is to be taken.

We note that any derivative of the form $\partial^n t_0 / \partial x^n$ $(n = 1, 2, 3, \ldots)$ satisfies (2.6), (2.3) and (2.4) and vanishes for $r \to \infty$. These solutions which satisfy homogeneous boundary conditions might be considered as eigenfunctions for the inner expansion. However, they do not satisfy (2.7), and infinite (non-integrable) heat-flux singularities exist at each end point. Appropriate eigenfunctions for the inner expansion will be introduced later.

Since (2.8) does not satisfy the boundary condition at infinity, an outer solution, valid for $r \to \infty$, is required.

Formulation of first- and second-order outer problems

In the outer region where $r \gg 1$ it is convenient to consider the limit $\epsilon \to 0$ to be a result of letting $L \to 0$. Since an infinitesimal strip with finite heat flux cannot be expected to alter the temperature at infinity, the first-order outer solution, satisfying (2.2) and (2.5), is simply

$$T(X, Y) = 1,$$

where X and Y are outer variables defined by

$$X = \epsilon^{\alpha} x, \quad Y = \epsilon^{\beta} y, \tag{2.9}$$

and $\alpha, \beta > 0$ are constants which will now be determined.

If the change of variable (2.9) is introduced into (2.2), there are several possible choices of α and β which lead to different partial differential equations. However, the particular choice $\alpha = \beta = \frac{1}{2}$ leads to a distinguished limit for which the governing equation is the same as (2.2) with $\epsilon \equiv 1$, i.e.

$$Y \, \partial T / \partial X = \nabla^2 T, \tag{2.10}$$

where now the Laplacian is with respect to (X, Y). Although the equation is not simplified in the outer region, there is a significant change in the boundary conditions because the strip now appears as a point sink located at the origin $R = (X^2 + Y^2)^{\frac{1}{2}} = 0$; therefore it will be necessary to satisfy only matching conditions for $R \to 0$ rather than the exact boundary condition (2.3).

To obtain the second approximation we write

$$T \sim 1 + f(\epsilon) T_1(X, Y), \tag{2.11}$$

where the gauge function $f(\epsilon)$ will be determined by the matching procedure. Substituting (2.11) into (2.10), we obtain (2.10) with T replaced by T_1.

Boundary conditions

The boundary conditions (2.4) and (2.5) will be satisfied provided that

$$\partial T_1 / \partial Y = 0 \quad \text{for} \quad Y = 0, \quad |X| > 0 \tag{2.12}$$

and

$$T_1 \to 0 \quad \text{for} \quad R = (X^2 + Y^2)^{\frac{1}{2}} \to \infty. \tag{2.13}$$

At the origin the sink condition requires

$$T_1 \sim (k/\pi)\ln R \quad \text{for} \quad R \to 0. \tag{2.14}$$

The half-sink strength k can be absorbed into the gauge function $f(\epsilon)$ and will be determined later.

The singularity condition (2.14) holds on the boundary of the domain and it is convenient to combine (2.12) and (2.14) into a single condition along $Y = 0+$ by applying the divergence theorem to (2.10) over the area of a thin rectangle specified as follows: the lower edge coincides with the X axis but is indented above the origin $R = 0$ via a small semicircle of radius ϵ', the side parallel to this is at a distance $Y = \delta > \epsilon' > 0$ and the other pair of parallel sides are at $X = \pm M$. Using (2.12) and (2.14) and assuming that the contributions from the integrals along $X = \pm M$ vanish when $M \to \infty$ and $\delta \to 0$,† we recover after letting $\delta \to 0$

$$\int_{-\infty}^{\infty} \left[\frac{\partial T_1}{\partial Y}\right]_{Y=0+} dX = k. \tag{2.15}$$

Conditions (2.12) and (2.14) will now be satisfied by taking

$$[\partial T_1/\partial Y]_{Y=0+} = k\delta(X) \quad (-\infty < X < \infty), \tag{2.16}$$

which is consistent with (2.15).

3. Determination of $T_1(X, Y)$

To solve (2.10) subject to (2.13) and (2.16), we introduce the Fourier transform and its inverse, i.e.

$$\psi(\alpha, Y) = \int_{-\infty}^{\infty} T_1(X, Y) e^{i\alpha X} dX, \qquad T_1(X, Y) = \frac{1}{2\pi}\int_{-\infty}^{\infty} \psi(\alpha, Y) e^{-i\alpha X} d\alpha. \tag{3.1}$$

After taking the transform of (2.10) and letting

$$s = e^{-\frac{1}{6}\pi i}\alpha^{\frac{1}{3}}(Y + i\alpha), \tag{3.2}$$

we obtain Airy's equation

$$d^2\psi/ds^2 - s\psi = 0. \tag{3.3}$$

The solution of (3.3) which satisfies (2.13) is given by

$$\psi(s, Y) = H(\alpha)\,\mathrm{Ai}\,(s) \tag{3.4}$$

provided that $|\arg s| < \frac{1}{3}\pi$, which requires $-\frac{1}{2}\pi < \arg\alpha < \frac{3}{2}\pi$. Therefore a branch cut must be introduced along the negative imaginary axis in the α plane.

To determine $H(\alpha)$ we take the transform of (2.16) and use (3.4); thus

$$H(\alpha) = k e^{\frac{1}{6}\pi i}/\alpha^{\frac{1}{3}}\,\mathrm{Ai}'\,(s_0), \tag{3.5}$$

where $s_0 = s|_{Y=0} = e^{\frac{1}{3}\pi i}\alpha^{\frac{2}{3}}$ and the prime denotes differentiation with respect to the argument. Using the inversion integral, we find

$$T_1(X, Y) = \frac{k}{2\pi} e^{\frac{1}{6}\pi i}\int_{-\infty}^{\infty} \frac{\mathrm{Ai}\,(s)}{\alpha^{\frac{1}{3}}\,\mathrm{Ai}'\,(s_0)} e^{-i\alpha X} d\alpha. \tag{3.6}$$

† These conditions can be verified *a posteriori*.

For $X < 0$ we evaluate (3.6) by considering a contour integral which is closed in the upper half-plane. The function $\mathrm{Ai}'(s_0)$ has simple zeros when $\alpha = i\rho_n^{\frac{3}{2}}$, where

$$\mathrm{Ai}'(-\rho_n) = 0 \quad (\rho_n > 0, n = 1, 2, 3, \ldots).$$

Using the calculus of residues we find

$$T_1(X, Y) = -\tfrac{3}{4}k \sum_{n=1}^{\infty} \frac{\mathrm{Ai}[\rho_n^{\frac{1}{3}}(Y-\rho_n^{\frac{3}{2}})]}{\rho_n^{\frac{3}{2}}\,\mathrm{Ai}(-\rho_n)} \exp(\rho_n^{\frac{3}{2}} X) \quad \text{for} \quad X \leqslant 0. \tag{3.7}$$

For $X > 0$ we consider a contour integral in the lower half-plane which embraces the branch line along the negative imaginary axis. After some algebra we obtain

$$T_1(X, Y) = \frac{k}{\pi} \mathrm{Re} \int_0^{\infty} \frac{e^{-\frac{1}{6}\pi i}\,\mathrm{Ai}[e^{-\frac{1}{3}\pi i} r^{\frac{1}{3}}(Y+r)]}{r^{\frac{1}{3}}\,\mathrm{Ai}'(e^{-\frac{1}{3}\pi i} r^{\frac{2}{3}})} e^{-rX}\, dr \quad \text{for} \quad X \geqslant 0. \tag{3.8}$$

Asymptotic expansion for $R \to 0$

To carry out the matching we require an asymptotic expansion of $T_1(X, Y)$ for $R \to 0$. It is sufficient (and convenient) to use the solution (3.8), valid for $X \geqslant 0$, for this purpose. Since the integral in (3.8) and its X and Y derivatives are marginally convergent when $X, Y \to 0$, some careful manipulations are required to extract the required information. We rewrite (3.8) in the following way:

$$\begin{aligned} \frac{\pi}{k} T_1(X, Y) = \mathrm{Re} \int_0^1 & \frac{e^{-\frac{1}{6}\pi i}\,\mathrm{Ai}(s)}{r^{\frac{1}{3}}\,\mathrm{Ai}'(s_0)} e^{-rX}\, dr \\ & + \mathrm{Re} \int_1^{\infty} \left[\frac{e^{-\frac{1}{6}\pi i}\,\mathrm{Ai}(s)}{r^{\frac{1}{3}}\,\mathrm{Ai}'(s_0)} e^{-rX} + \frac{\exp(\frac{1}{4}iY^2 - r\bar{Z})}{r} \left(1 + \frac{F(Y)}{r} + \frac{G(Y)}{r^2}\right) \right] dr \\ & - \mathrm{Re}\{\exp(\tfrac{1}{4}iY^2)[E_1(\bar{Z}) + F(Y)\,E_2(\bar{Z}) + G(Y)\,E_3(\bar{Z})]\}, \end{aligned} \tag{3.9}$$

where now $s = e^{-\frac{1}{3}\pi i} r^{\frac{1}{3}}(Y+r)$, $s_0 = s|_{Y=0}$, $\bar{Z} = X - iY$,

$$F(Y) = -\tfrac{1}{4}(Y + \tfrac{1}{6}iY^3),$$

$$G(Y) = \tfrac{1}{4}(-i + \tfrac{5}{8}Y^2 + \tfrac{1}{24}iY^4 - \tfrac{1}{288}Y^6),$$

and $E_n(u)$ is the exponential integral, defined by

$$E_n(u) = \int_1^{\infty} t^{-n} e^{-ut}\, dt.$$

The infinite integral in (3.9) and its first and second partial derivatives with respect to X and Y are now uniformly convergent for $X, Y \geqslant 0$. The functions $F(Y)$ and $G(Y)$ are determined from the asymptotic expansion of $\mathrm{Ai}(s)/\mathrm{Ai}'(s_0)$ for $r \to \infty$. When (3.9) is evaluated for $R \to 0$ we find

$$(\pi/k)\, T_1 \sim \ln R + a_0 + a_1 X + a_2 Y - \tfrac{1}{8}(X^2 - Y^2)\theta + a_3 X^2 + a_4 XY + a_5 Y^2 + \ldots, \dagger \tag{3.10}$$

† The asymmetric term $(X^2 - Y^2)\theta$ is not harmonic and is a direct result of convection.

where $$a_0 = \gamma + \frac{3}{4}\left\{\int_0^1 \frac{\mathrm{Ai}(X)}{\mathrm{Ai}'(X)}\frac{dX}{X^{\frac{1}{2}}} + \int_1^\infty \left[\frac{\mathrm{Ai}(X)}{\mathrm{Ai}'(X)}\frac{1}{X^{\frac{1}{2}}} + \frac{1}{X}\right] dX\right\} = -1{\cdot}0559\ldots,\dagger$$

$$a_1 = -\tfrac{3}{4}\cos\left(\frac{\pi}{4}\right)\int_0^\infty \left(X^{\frac{1}{2}}\frac{\mathrm{Ai}(X)}{\mathrm{Ai}'(X)} + \frac{1}{X^{\frac{1}{2}}}\right) dX = -0{\cdot}4176\ldots,\dagger$$

$$a_2 = 0, \quad a_3 = \tfrac{1}{32}\pi, \quad a_4 = \tfrac{1}{8}, \quad a_5 = -\tfrac{1}{32}\pi$$

and $\theta = \tan^{-1}(Y/X)$ is in the range $0 \leqslant \theta \leqslant \pi$. In obtaining a_0, a_1, a_3 and a_5 from (3.9) it is necessary to evaluate integrals along an infinite ray with argument $(-\frac{1}{3}\pi)$ which are displaced to the positive real axis using contour integration. The details of these calculations are not trivial but they are too lengthy to reproduce here.

First-order matching

Expanding the first-order inner solution (2.8) for $|z| \to \infty$, we obtain

$$T = g(\epsilon)\,[\ln r + \ln 2 + O(r^{-2})]. \tag{3.11}$$

Using (2.9) and (3.10) we consider the limit $R \to 0$ of the two-term outer expansion (2.11), and express the result in terms of the inner variables, i.e.

$$T = 1 + (k/\pi)f(\epsilon)\,[\ln \epsilon^{\frac{1}{2}} + \ln r + a_0 + O(\epsilon^{\frac{1}{2}})]. \tag{3.12}$$

By choosing
$$g(\epsilon) = (k/\pi)f(\epsilon) = [\ln(2/\epsilon^{\frac{1}{2}}) - a_0]^{-1}, \tag{3.13}$$

the terms displayed in (3.11) and (3.12) will be matched with an error $O(\epsilon^{\frac{1}{2}} g(\epsilon))$. The neglected terms will be matched when higher-order terms in the inner and outer expansion are considered.

4. The inner expansion

We shall assume and verify *a posteriori* that the inner expansion has the following form:
$$T(x, y) = g(\epsilon)\,\{t_0(x, y) + \epsilon^{\frac{1}{2}} t_1(x, y) + \epsilon t_2(x, y) + \epsilon g(\epsilon)\, t_3(x, y) + o[\epsilon g(\epsilon)]\}, \tag{4.1}$$

where $g(\epsilon)$ is given by (3.13) and $t_0(x, y)$ by (2.8). We might expect that an asymptotic sequence of the form $\{g(\epsilon)\}^n$ $(n = 1, 2, 3, \ldots)$ would be required in this problem on the basis of the resolution of the Stokes paradox for the two-dimensional low Reynolds number flow past a circular cylinder given by Kaplun (1957) and Proudman & Pearson (1957). The critical difference there is the nonlinearity of the Navier–Stokes equation, which compounds the inverse powers of the logarithm; thus the convection terms which are $O(\epsilon)$ will not enter that asymptotic expansion until all the inverse powers of the logarithms have been disposed of. In our problem the convective terms enter the inner expansion at the third order owing to the linearity of the governing equations.

The term $t_1(x, y)$

The term $O(X)$ in (3.10) requires that a term $O(\epsilon^{\frac{1}{2}} g(\epsilon))$ should appear in the inner expansion for the matching to be carried out successfully. By substituting (4.1) into (2.2) we find
$$\nabla^2 t_1 = 0, \tag{4.2}$$

and t_1 must satisfy the boundary conditions (2.3) and (2.4) and asymptote to $a_1 x$ for $r \to \infty$.

† These constants were determined by numerical integration.

Inner eigenfunctions

There exists a set of harmonic functions which satisfy (2.3), (2.4) and (2.7) and which grow algebraically for $r \to \infty$. These functions are given by any real multiple of the functions

$$e_n(x, y) = \mathrm{Re}\{[z + (z^2-1)^{\frac{1}{2}}]^n - [z + (z^2-1)^{\frac{1}{2}}]^{-n}\} \quad (n = 1, 2, 3, \ldots), \tag{4.3}$$

where the branch of $(z^2-1)^{\frac{1}{2}}$ is defined as before. The solution for t_1 corresponds to the case $n = 1$ and the matching determines the multiplicative constant. For now we write

$$t_1(x, y) = C_1 e_1(x, y), \tag{4.4}$$

and C_1 will be determined later.

The term $t_2(x, y)$

The equation satisfied by t_2 is

$$\nabla^2 t_2 = y\, \partial t_0/\partial x. \tag{4.5}$$

To find a particular solution t_{21}, we formally introduce new independent variables $z = x + iy$ and $\bar{z} = x - iy$. When (4.5) is transformed in this way we find

$$\partial^2 t_{21}/\partial z\, \partial \bar{z} = (16i)^{-1}(z - \bar{z})[(z^2-1)^{-\frac{1}{2}} + (\bar{z}^2-1)^{-\frac{1}{2}}], \tag{4.6}$$

where (2.8) has been used to evaluate the right-hand side. A straightforward integration yields

$$t_{21}(x, y) = \tfrac{1}{16}\,\mathrm{Im}\{2\bar{z}(z^2-1)^{\frac{1}{2}} - \bar{z}^2 \ln[z + (z^2-1)^{\frac{1}{2}}]\}. \tag{4.7}$$

We now determine a harmonic function t_{22} which assumes the value $[-\partial t_{21}/\partial y]_{y=0}$ for $|x| > 1$ on $y = 0$. This function is readily found to be

$$t_{22}(x, y) = -\tfrac{1}{16}\,\mathrm{Im}\{(z^2+1)\ln[z + (z^2-1)^{\frac{1}{2}}] - z(z^2-1)^{\frac{1}{2}}\}. \tag{4.8}$$

Finally, to satisfy (2.3) we require another harmonic function t_{23} which takes on the values

$$\begin{aligned} t_{23}(x, 0) &= -t_{21}(x, 0) - t_{22}(x, 0) \\ &= -\tfrac{1}{16}\{3x(1-x^2)^{\frac{1}{2}} - (2x^2+1)\tan^{-1}[(1-x^2)^{\frac{1}{2}}/x]\} \quad \text{for} \quad |x| < 1, \end{aligned} \tag{4.9}$$

$$[\partial t_{23}/\partial y]_{y=0} = 0 \quad \text{for} \quad |x| > 1, \tag{4.10}$$

and

$$|t_{23}| < \infty \quad \text{for} \quad r \to \infty, \tag{4.11}$$

where the inverse tangent in (4.9) is chosen in the range $[0, \pi]$.

This potential problem may be solved by mapping the upper half-plane into a semi-infinite strip in the ζ plane shown in figure 2. The required transformation is

$$z = \sin(\tfrac{1}{2}\pi\zeta) \quad (\zeta = \xi + i\eta) \tag{4.12}$$

and the problem becomes

$$\nabla'^2 t_{23} = 0 \quad \text{for} \quad |\xi| \leqslant 1, \quad \eta \geqslant 0, \tag{4.13}$$

$$t_{23}(\xi, 0) = -\tfrac{1}{32}[3\sin\pi\xi + \pi\xi(2 - \cos\pi\xi)] + \tfrac{1}{32}\pi(2 - \cos\pi\xi)] \quad \text{for} \quad |\xi| \leqslant 1, \tag{4.14}$$

$$\partial t_{23}/\partial\xi = 0 \quad \text{for} \quad \xi = \pm 1, \quad \eta \geqslant 0, \tag{4.15}$$

$$|t_{23}| < \infty \quad \text{for} \quad \eta \to \infty, \quad |\xi| \leqslant 1, \tag{4.16}$$

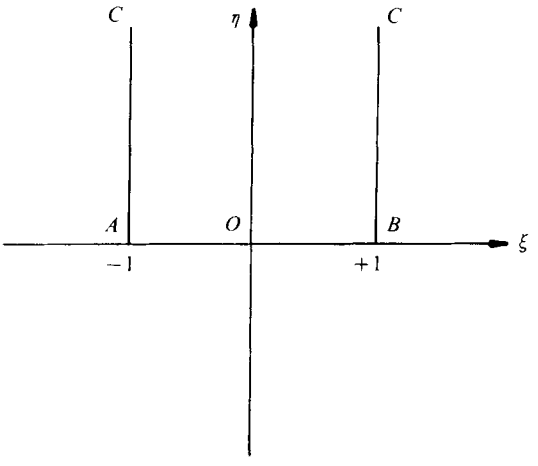

FIGURE 2. The ζ plane.

where ∇'^2 is the Laplacian with respect to (ξ, η). The solution is obtained by use of Fourier series and is given by

$$t_{23}(\xi,\eta) = -\frac{8}{\pi}\sum_{n=0}^{\infty}(-1)^n B_n\, e^{-\frac{1}{2}(2n+1)\pi\eta}\sin\left(\frac{2n+1}{2}\pi\xi\right) + \frac{\pi}{32}(2 - e^{-\pi\eta}\cos\pi\xi), \tag{4.17}$$

where $B_n = [(2n-1)\,(2n+1)\,(2n+3)]^{-2}$.

The solution for t_2 can now be written as

$$t_2(x,y) = t_{21}(x,y) + t_{22}(x,y) + t_{23}(x,y) + C_2\, e_2(x,y), \tag{4.18}$$

where the multiple of the eigenfunction C_2 will be determined by the matching. Note that only a multiple of e_2 is required at this stage to match the quadratic terms which appear in (3.10).

5. Detailed matching procedure and higher-order terms in the outer expansion

We now apply the limit $r \to \infty$ to the first three terms of the inner expansion and express the result in terms of the outer variables using (2.9); thus

$$\begin{aligned} T = g(\epsilon)\{&\ln 2R - \ln\epsilon^{\frac{1}{2}} + 2C_1 X + 4C_2(X^2 - Y^2) + a_4 XY - \tfrac{1}{8}(X^2 - Y^2)\theta \\ &+ \tfrac{1}{4}\epsilon[-R^{-2}\cos 2\theta - 4C_1 R^{-1}\cos\theta - \tfrac{1}{4}\theta + \tfrac{1}{4}\sin 2\theta - \tfrac{1}{8}\sin 2\theta\cos 2\theta - 8C_2 \\ &+ \tfrac{1}{4}\pi] + o(\epsilon)\}. \end{aligned} \tag{5.1}$$

It should be noted that, although $t_{23} = \frac{1}{16}\pi + O(e^{-\frac{1}{2}\pi\eta})$ when $\eta \to \infty$, we do not obtain exponential decay in the z plane. In fact, $t_{23} = \frac{1}{16}\pi + O(r^{-1})$ but this does not alter the results above until terms $O(\epsilon^{\frac{3}{2}})$ are included in the curly brackets.

We now take the limit $R \to 0$ of the two-term outer expansion (2.11), i.e.

$$T = g(\epsilon)\{\ln 2R - \ln\epsilon^{\frac{1}{2}} + a_1 X + a_3(X^2 - Y^2) + a_4 XY - \tfrac{1}{8}(X^2 - Y^2)\theta + O(\text{cubic terms})\}. \tag{5.2}$$

The neglected cubic terms in (5.2) will have to be matched to terms $O[\epsilon^{\frac{3}{2}} g(\epsilon)]$ in the inner expansion. It can now be seen that all terms $O[g(\epsilon)]$ will be matched in (5.1) and (5.2) provided that we choose the multiples of the eigenfunctions such that

$$C_1 = \tfrac{1}{2}a_1, \quad C_2 = \tfrac{1}{4}a_3. \tag{5.3}$$

The remaining terms in (5.1), which are $O[\epsilon g(\epsilon)]$, can now be used to deduce the forms of the third and fourth terms in the outer expansion.

Eigenfunctions for the outer expansion

We observe that the functions

$$h_n(X, Y) = \partial^n T_1 / \partial X^n \tag{5.4}$$

satisfy (2.10), (2.12) and (2.13) and behave like $\partial^n (\ln R)/\partial X^n$ for $R \to 0$. These are the eigenfunctions of the outer expansion. For $n = 1, 2$, the behaviour at the origin is given by

$$\frac{\partial}{\partial X} \ln R = \frac{\cos\theta}{R}, \quad \frac{\partial^2}{\partial X^2} \ln R = -\frac{\cos 2\theta}{R^2}.$$

When these terms are compared with the first two terms in the square brackets of (5.1), it is readily inferred that the outer expansion should contain the terms

$$\tfrac{1}{4}\epsilon g(\epsilon)\,(\partial^2 T_1/\partial X^2 - 2a_1\,\partial T_1/\partial X). \tag{5.5}$$

If these additional terms in the outer expansion are evaluated for $R \to 0$, we find that all of the terms in the square brackets of (5.1) will be matched except for the constant terms, which must obey the equation

$$-8C_2 + \tfrac{1}{4}\pi \equiv -2a_3 + \tfrac{1}{4}\pi \stackrel{?}{=} 2a_3 - 2a_1^2,$$

or if equality holds,

$$\pi = -16a_1^2 < 0, \tag{5.6}$$

which is clearly impossible. This inconsistency is resolved by introducing the fourth-order term in the outer expansion

$$A\epsilon[g(\epsilon)]^2 T_1(X, Y) \tag{5.7}$$

and the fourth-order term in the inner expansion

$$B\epsilon[g(\epsilon)]^2 t_0(x, y), \tag{5.8}$$

where A and B are constants. When $r \to \infty$, the new term given by (5.8) introduces a constant term $O[\epsilon g(\epsilon)]$ in the expansion (5.1). By choosing A and B appropriately the inconsistency (5.6) can be removed, and the new heat flux established by the logarithmic divergence of t_0 in (5.8) will just match the logarithmic singularity of T_1 in (5.7) at the origin. After some algebra we find

$$A = B = -(a_3 + \tfrac{1}{2}a_1^2).$$

The introduction of these new terms will not affect any terms which have already been matched. The outer expansion can now be written as

$$T = 1 + g(\epsilon)\{T_1(X, Y) + \tfrac{1}{4}\epsilon(\partial^2 T_1/\partial X^2 - 2a_1\,\partial T_1/\partial X) - \epsilon g(\epsilon)\,(a_3 + \tfrac{1}{2}a_1^2)\,T_1(X, Y) + o[\epsilon g(\epsilon)]\}, \tag{5.9}$$

and for the inner expansion (4.1)

$$t_3(x, y) = -(a_3 + \tfrac{1}{2}a_1^2)\,t_0(x, y). \tag{5.10}$$

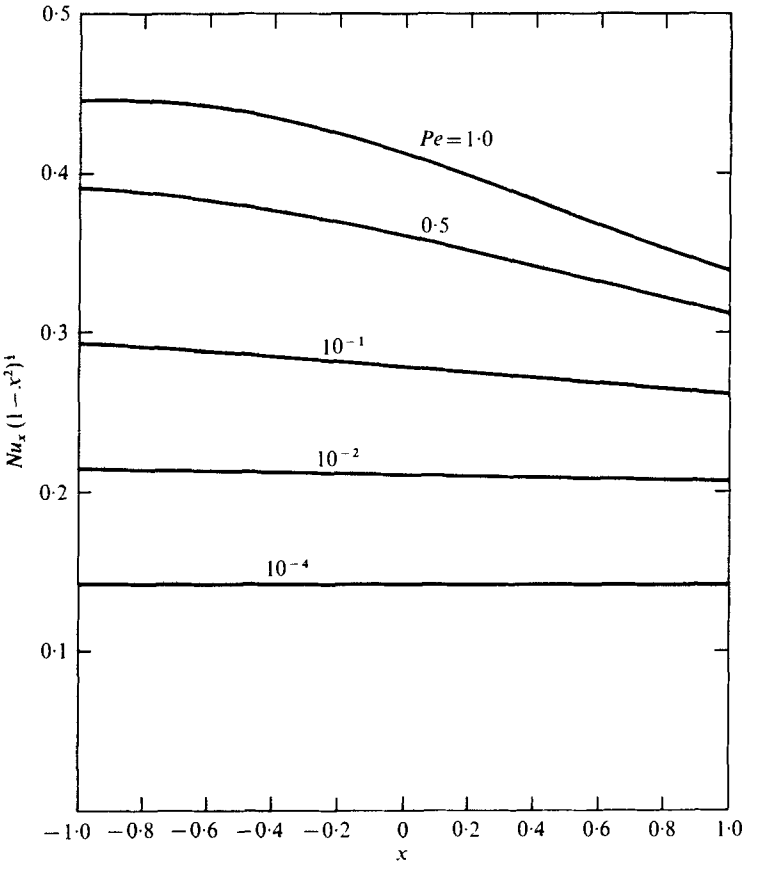

FIGURE 3. Theoretical local heat-transfer rate Nu_x *vs.* x for various values of Pe.

6. Heat flux from the plate

The absolute value of the local non-dimensional heat flux $q(x)$ is a local Nusselt number and is given by

$$Nu_x = [\partial T/\partial y]_{y=0} = (1-x^2)^{-\frac{1}{2}}\, g(\epsilon)\{1+\epsilon^{\frac{1}{2}}\alpha_1(x)+\epsilon\alpha_2(x)+\epsilon g(\epsilon)\,\alpha_3+o[\epsilon g(\epsilon)]\}, \quad (6.1)$$

where $\alpha_1(x) = a_1 x$, $\alpha_3 = -(a_3 + \frac{1}{2}a_1^2) = -0{\cdot}1853\ldots$,

$$\alpha_2(x) = a_3(1-2x^2) + \frac{8}{\pi}\sum_{n=0}^{\infty}(-1)^n(2n+1)\,B_n \sin[(2n+1)\sin^{-1}x]$$

and $|\sin^{-1}x| < \frac{1}{2}\pi$. In obtaining $\alpha_2(x)$ it is necessary to use the transformation

$$\left.\frac{\partial t_{23}(x,y)}{\partial y}\right|_{y=0} = \frac{2}{\pi(1-x^2)^{\frac{1}{2}}}\left.\frac{\partial t_{23}(\xi,\eta)}{\partial \eta}\right|_{\eta=0}.$$

The function $(1-x^2)^{\frac{1}{2}}Nu_x$ is displayed in figure 3 for several values of $Pe = 4\epsilon$. We should note that, although the factor $(1-x^2)^{\frac{1}{2}}$ is symmetric about $x = 0$, the function $(1-x^2)^{\frac{1}{2}}Nu_x$ is skewed, with larger values towards $x = -1$. This asymmetry is a result of the heat transfer from the front of the strip, which effectively reduces the temperature gradient available for heat transfer to the rear portion.

The integrated non-dimensional heat flux from the strip, i.e. the overall Nusselt number, results from only the first and fourth terms in the curly brackets of (6.1). These terms arise from the multiples of $t_0(x, y)$ in the inner expansion. We find

$$Nu_L = \int_{-1}^{1} Nu_x\, dx = \pi g(\epsilon)\{1 + \alpha_3 \epsilon g(\epsilon) + o[\epsilon g(\epsilon)]\}. \tag{6.2}$$

The one- and two-term results are shown *vs.* $Pe^{\frac{1}{2}}$ in figure 6 (see § 9), and the transition from small Pe to large Pe is surprisingly smooth. We have also displayed Springer's results and a correlation due to Newman (1973). In both cases there is fair agreement with our asymptotic theory provided that $Pe > 10^{-1}$. Of course the region $Pe = O(1)$ falls outside the range of any known theory, but the smooth transition from small to large Pe shown in figure 6 leaves little doubt as to how to estimate Nu for any Pe.

If the problem is such that the integrated dimensional heat flux $\bar{Q}$ from the strip is specified, as for a heated element, the temperature of the strip is given by

$$T_0 = T_\infty + (\bar{Q}/\kappa)\{\pi g(\epsilon)[1 + \alpha_3 \epsilon g(\epsilon)]\}^{-1}, \tag{6.3}$$

where the sign of $\bar{Q}$ must be chosen appropriately, depending on whether $T_0 \gtrless T_\infty$.

7. Temperature distribution far downstream in the wake

The solution in the wake may be found from (2.11) and (3.8) when $X \to \infty$. When X is large, the main contributions to the integral (3.8) result from small r. To obtain a solution uniformly valid in Y, we expand the integrand in a Taylor series as follows:

$$\mathrm{Ai}\,[e^{-\frac{1}{3}\pi i} r^{\frac{1}{3}}(Y + r)] \approx \mathrm{Ai}\,(e^{-\frac{1}{3}\pi i} r^{\frac{1}{3}} Y) + e^{-\frac{1}{3}\pi i} r^{\frac{4}{3}}\, \mathrm{Ai}'\,(e^{-\frac{1}{3}\pi i} r^{\frac{1}{3}} Y) + \ldots,$$

$$\mathrm{Ai}'\,(e^{-\frac{1}{3}\pi i} r^{\frac{4}{3}}) \approx \mathrm{Ai}'\,(0) + \tfrac{1}{2} e^{-\frac{2}{3}\pi i} r^{\frac{8}{3}}\, \mathrm{Ai}'''\,(0) + \ldots.$$

Substituting these results in (3.8) and retaining only the first-order terms, we find

$$T \sim 1 + \frac{g(\epsilon)}{\mathrm{Ai}'\,(0)} \mathrm{Re} \int_0^\infty \frac{e^{-\frac{1}{6}\pi i}\, \mathrm{Ai}\,(e^{-\frac{1}{3}\pi i} r^{\frac{1}{3}} Y)}{r^{\frac{1}{3}}} e^{-rX}\, dr.$$

We now make the substitutions $s = rX$ and $\eta = Y/X^{\frac{1}{3}}$ and find

$$T \sim 1 + \frac{g(\epsilon)}{\mathrm{Ai}'\,(0)} \frac{1}{X^{\frac{2}{3}}} \mathrm{Re} \int_0^\infty \frac{e^{-\frac{1}{6}\pi i}\, \mathrm{Ai}\,(e^{-\frac{1}{3}\pi i} \eta s^{\frac{1}{3}})\, e^{-s}}{s^{\frac{1}{3}}} ds. \tag{7.1}$$

The following identities, which have been obtained from Lebedev (1965, pp. 109 and 137), must now be used:

$$\mathrm{Ai}\,(z) = \tfrac{1}{3} z^{\frac{1}{2}}[I_{-\frac{1}{3}}(\zeta) - I_{\frac{1}{3}}(\zeta)], \quad \zeta = \tfrac{2}{3} z^{\frac{3}{2}}, \quad |\arg z| < \tfrac{2}{3}\pi,$$

$$I_\nu(\zeta) = e^{-\frac{1}{2}\nu\pi i} J_\nu(\zeta e^{\frac{1}{2}\pi i}), \quad -\pi < \arg \zeta \leqslant \tfrac{1}{2}\pi.$$

When these results are substituted in (7.1) we find

$$T \sim 1 + \frac{g(\epsilon)}{\mathrm{Ai}'\,(0)} \frac{\cos\,(\frac{1}{6}\pi)}{3} \frac{\eta^{\frac{1}{2}}}{X^{\frac{2}{3}}} \int_0^\infty s^{-\frac{1}{6}} J_{-\frac{1}{3}}(\tfrac{2}{3} s^{\frac{1}{2}} \eta^{\frac{3}{2}})\, e^{-s}\, ds. \tag{7.2}$$

If we now put $s = u^2$ we obtain

$$T \sim 1 + \frac{2}{3} \frac{g(\epsilon) \cos\,(\frac{1}{6}\pi)}{\mathrm{Ai}'\,(0)} \frac{\eta^{\frac{1}{2}}}{X^{\frac{2}{3}}} \int_0^\infty u^{\frac{2}{3}} J_{-\frac{1}{3}}(au) \exp\,(-u^2)\, du,$$

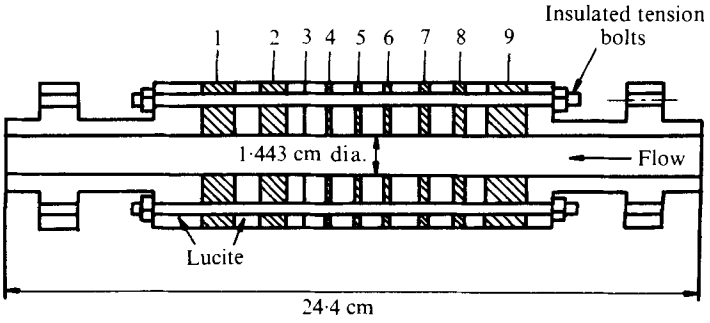

FIGURE 4. Experimental test section. Lengths of nickel electrodes (cm): (1) 0·000158; (2) 0·357; (3) 0·00250; (4) 0·008; (5) 0·0151; (6) 0·0517; (7) 0·0781; (8) 0·169; (9) 0·547.

which can be evaluated in closed form. From Gradshteyn & Ryzhik (1965, p. 717) we find

$$T \sim 1 - \frac{3^{\frac{1}{2}}}{2}\Gamma(\tfrac{1}{3})g(\epsilon)\frac{\exp(-\frac{1}{9}\eta^3)}{X^{\frac{2}{3}}} \quad \text{for} \quad X \to \infty, \quad Y \geqslant 0. \tag{7.3}$$

We may compute the total flux from the plate by integrating the defect in flux crossing a line X = constant far downstream. Thus

$$Nu_L = \int_0^\infty (1-T)\, Y\, dY = \pi g(\epsilon),$$

which is in agreement with the first-order result in (6.2).

8. Experimental technique

The theoretical results were verified by obtaining experimental data on mass-transfer to a liquid flowing in a horizontal tube using the well-known diffusion-controlled electrode or 'limiting-current' technique (see, for example, Eisenberg, Tobias & Wilke 1954; Patel, McFeeley & Jolls 1975). Mass-transfer measurements offer advantages over heat-transfer measurements in that the Schmidt number for liquids is very large (in contrast to the Prandtl number), which justifies the assumption of a linear velocity profile within the thin concentration boundary layer.

The experiments were performed in a flow loop (similar to that of Patel *et al.* 1975) of PVC pipe (inside diameter 1·443 cm) in which was placed the test section, consisting of nine nickel electrodes (see figure 4). The test section was located 175 pipe diameters from the entrance of the pipe, where a bundle of 26 Teflon tubes (14 AWG, thin walled) served as a flow straightening section. In the range of tube Reynolds numbers used, the test section was located well beyond the laminar entrance region in the tube. The electrolyte solution was continuously circulated from a collection tank downstream of the test section to a constant-head tank and thence through the pipe to the test section. The solution was sparged with nitrogen and all liquid surfaces were kept under a nitrogen atmosphere to avoid dissolved oxygen, which can cause inaccurate results with the limiting-current method. The electrodes were mechanically and electrolytically cleaned from time to time to remove deposits and to prevent poisoning of the electrode surfaces.

c	bulk concentration (moles/l)	0·0086 to 0·01
ν	kinematic viscosity (cm²/s)	$1{\cdot}11 \times 10^{-2}$ to $1{\cdot}38 \times 10^{-2}$
T	temperature (°C)	20 to 30
Re	tube Reynolds number	0·42 to 1500
Pe	Péclet number	$1{\cdot}11 \times 10^{-4}$ to 5×10^{6}
Sc	Schmidt number	2650 to 2850

TABLE 1. Ranges of experimental variables.

The electrolyte consisted of an equimolar solution (approximately 0·01 M) of potassium ferrocyanide and potassium ferricyanide in de-ionized water with 2N sodium hydroxide as a supporting electrolyte. A particular solution was used for about five days and then discarded; thus solution properties varied somewhat for each series of runs. Table 1 gives the ranges of the relevant physical properties and flow parameters for all the runs.

A potential difference was imposed between one of the electrodes in the test section and a very large nickel electrode, immersed in the electrolyte upstream of the test section, which served as the anode. In the limiting-current region, the concentration of ferricyanide ions at the surface of the test electrode was essentially zero and the current in the circuit (measured with a current-measuring amplifier) gave the mass-transfer rate of ferricyanide ions to the test electrode surface. The bulk concentration of ferricyanide ions was determined by titration. The velocity gradient at the wall could be calculated from the assumed parabolic velocity distribution and a measurement of the volumetric flow rate.

The nine ring-shaped nickel electrodes were of various thicknesses and the inner edge of each ring was in contact with the electrolyte, thus presenting a different mass-transfer length in the flow direction. The advantage of such electrodes is that they are axisymmetric, and there will be no diffusion in the azimuthal direction. The effect of wall curvature could be neglected because of the very thin concentration boundary layer.

Each of electrodes 2–9 was cut from nickel stock, insulated by being coated with a thin film of nylon, applied by electrostatic spraying, and separated from its neighbours by disks of lucite. Electrode 1 was the smallest and was prepared by a different and rather novel technique, to be described later. Rubber O-rings (not shown in figure 4) were used between all mating surfaces and the entire assembly was held together by insulated tension bolts. Great care was taken to make the inside of the test section as smooth as possible.

Since low Péclet numbers were to be investigated, a very thin electrode was essential. We attempted to fabricate this electrode (electrode 1) by using thin nickel foil in the same manner as for electrodes 2–9, but the material was too fragile to make a suitable electrode. The technique finally developed was to make a disk of Rexolite (a cross-linked polystyrene which is heat resistant) of the required shape with a hole in its centre of the same diameter as the internal diameter of the test section. A mating Teflon plug was also made and fitted into this hole. A film of nickel, a few Ångstroms thick, was then vapour deposited on one of the flat surfaces of the disk. The Teflon plug prevented nickel from entering the centre hole. The original thin nickel layer was then built up in thickness by electrolytically depositing nickel on it with the plug still in place. When the plug was removed and the disk examined under a microscope,

it was found that the exposed edge of nickel was smooth and uniform. During vapour deposition the Rexolite experienced slight irreversible thermal expansion so it was necessary to increase slightly the internal diameters of the rest of the elements in the test section. The final internal diameter was 1·443 cm.

Electrode 2 and 4–9 were first tested by comparing data taken with them at large Péclet numbers (>1000) with the Leveque solution. Electrodes 1 and 3 could not be tested in this way because sufficiently high Péclet numbers could not be achieved in our apparatus owing to their small thicknesses and our limited liquid heads. Diffusion coefficients of the ferricyanide ion were obtained from the correlation of Gordon, Newman & Tobias (1966), which for the ionic concentrations used here is

$$\mathscr{D}\mu/T = 0{\cdot}234 \times 10^{-9}\,\mathrm{cm^2\,P/s\ ^\circ K},$$

where $\mathscr{D}$ is the diffusion coefficient (analogous to κ above), μ is the viscosity of the electrolyte and T is the absolute temperature. It was found that electrodes 2 and 9 (the two largest) gave results which differed from the Leveque solution by less than 10 % but the others gave transfer rates much lower than those predicted by the Leveque solution. After repeated cleaning, dismantling and re-assembly, remachining, etc. of the electrodes, the results were unchanged. It was concluded that the discrepancy arose either from inaccuracies in the thicknesses of the smaller electrodes or possibly because portions of the electrodes could be passive. The electrode lengths were therefore calibrated using the Leveque solution at large Péclet numbers. This procedure was checked by making other runs at different but large Péclet numbers to verify that the Leveque solution was obeyed. The agreement was excellent and justified the procedure used.

Electrodes 1 and 3 were calibrated using data from the other electrodes at lower Péclet numbers by an inverse method. By comparing the measured outputs of electrodes 1 and 3 with data from the others, their respective Péclet numbers were obtained and their lengths calculated. The procedure was checked using several runs and the agreement was excellent. The electrode lengths shown in figure 4 are the calibrated electrode lengths, rather than the measured lengths.

Once the electrodes had been calibrated, Nusselt numbers for various Péclet numbers were obtained by varying the solution flow rate and using various electrodes. Péclet numbers as low as $1{\cdot}15 \times 10^{-4}$ were achieved. It was difficult to obtain lower values because the low flow rates could not be carefully controlled. Nusselt and Péclet numbers were calculated from the formulae

$$Nu_L = I/\pi cD\mathscr{D}\mathscr{F}, \quad Pe = 32WL^2/\pi D^3\rho\mathscr{D},$$

where I is the limiting current, c is the bulk ferricyanide concentration, D is the pipe diameter, $\mathscr{F}$ is Faraday's constant, W is the mass flow rate of electrolyte and ρ is the electrolyte density. The measurement error in the Nusselt number is estimated to be less than 6 % and that in the Péclet number to be less than 7 %.

9. Discussion of results

Experimental data points are displayed in figure 5 for $Pe < 10$. It is remarkable that the data fall so near the theoretical curve for $Pe \leqslant 4$ when the asymptotic theory on which it is based is valid for $Pe \to 0$.

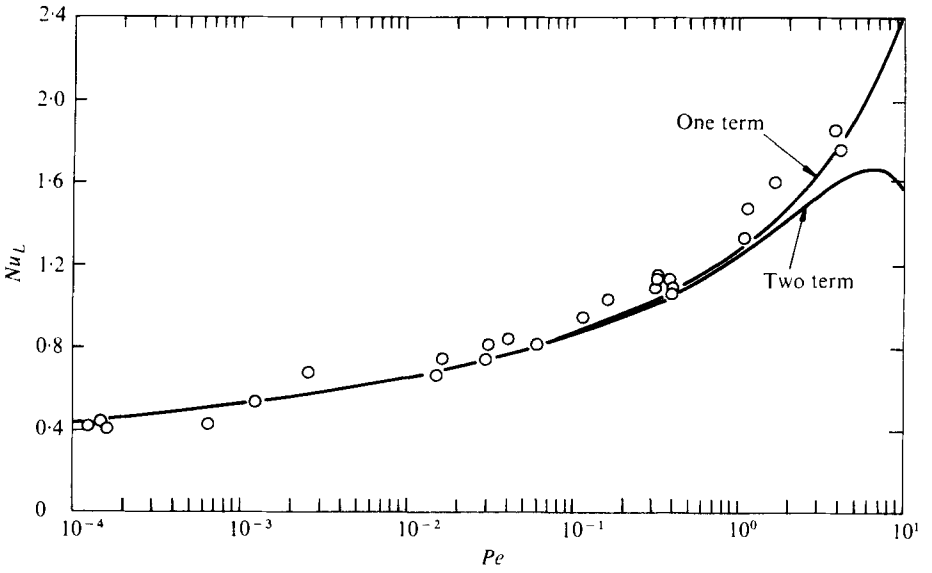

FIGURE 5. Theoretical overall heat-transfer rate Nu_L *vs.* Pe and experimental data points for $10^{-4} < Pe < 10$.

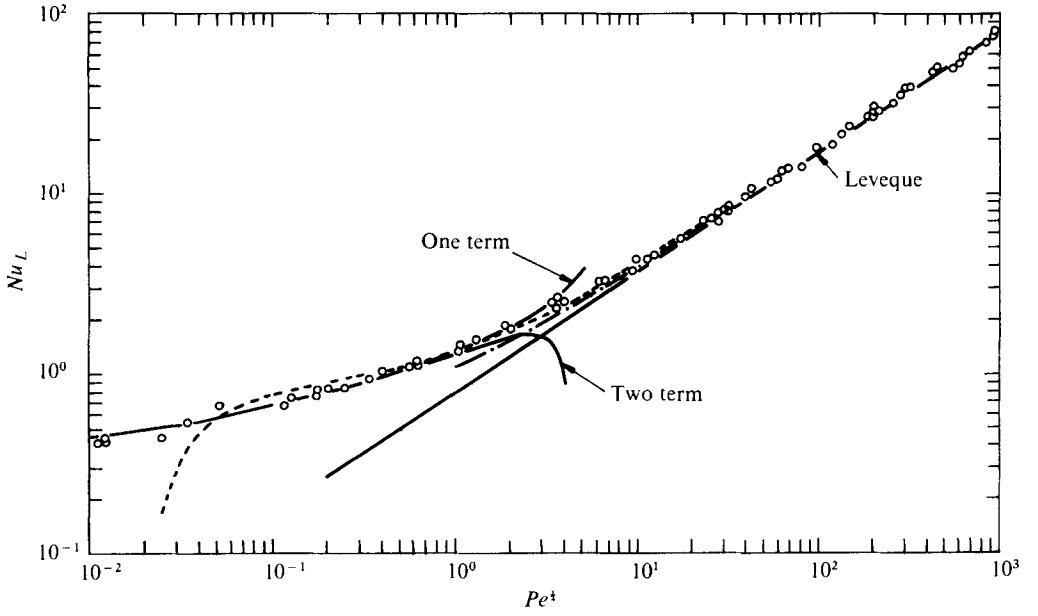

FIGURE 6. Overall heat-transfer rate Nu_L *vs.* $Pe^{\frac{1}{2}}$ for all investigators with experimental data for $10^{-4} < Pe < 10^{6}$. ——, present work and Leveque solution; – – –, Newman; –·–, Springer; ○, experimental points.

To display the experimental data over a larger range of Pe, we have chosen $Pe^{\frac{1}{2}}$ as the abscissa in figure 6. The agreement with the various theoretical curves over 8 decades of the Péclet number is very good. Although a few of the data points for large values of Pe were used to calibrate the probe lengths (see § 8), additional experimental points were obtained for large Pe and these agree very well with the Leveque solution.

In the region $4 < Pe < 400$ the experimental points fall above values from Newman's correlation and Springer's results. Although this is not easily seen from figure 6, owing to the scale used, Newman's correlation is in better agreement with the data in this range.

In conclusion, we have obtained excellent agreement between our asymptotic theory, which is valid for $Pe \to 0$ and which describes the steady heat/mass transfer from a strip in a uniform shear flow, and experimental data obtained from an experiment which covers a much larger range of Péclet numbers. From the results presented here and the work of others, it is now possible to predict the Nusselt number for *any* value of the Péclet number.

We hope to apply these results to shear flows with a small time-periodic component when the Péclet number is small. It may also be possible to use the methods presented here to determine the heat/mass transfer to objects of different shapes placed in a uniform shear flow.

The authors are grateful for the support provided by the National Science Foundation under Grant ENG 75-20863.

REFERENCES

EISENBERG, M., TOBIAS, C. W. & WILKE, C. R. 1954 Ionic mass transfer and concentration polarization at rotating electrodes. *J. Electrochem. Soc.* **101**, 306.

GORDON, S. L., NEWMAN, J. S. & TOBIAS, C. W. 1966 The role of ionic migration in electrolytic mass transport; diffusivities of $[Fe(CN)_6]^{3-}$ and $[Fe(CN)_6]^{4-}$ in KOH and NaOH solutions. *Ber. Bunsenges. Phys. Chem.* **70**, 414.

GRADSHTEYN, I. S. & RYZHIK, I. M. 1965 *Tables of Integrals, Series and Products.* Academic Press.

KAPLUN, S. 1957 Low Reynolds number flow past a circular cylinder. *J. Math. Mech.* **6**, 595.

LEBEDEV, N. N. 1965 *Special Functions and Their Applications.* Dover.

LEVEQUE, M. A. 1928 Transmission de chaleur par convection. *Ann. Mines* **13**, 283.

LING, S. C. 1963 Heat transfer from a small isothermal spanwise strip in an insulated boundary. *J. Heat Transfer, Trans. A.S.M.E.* C **85**, 230.

NEWMAN, J. 1973 The fundamental principles of current distribution and mass transport in electrochemical cells. In *Electroanalytical Chemistry* (ed. Allen J. Bard), vol. 6, p. 187. Marcel Dekker.

PATEL, R. D., MCFEELEY, J. J. & JOLLS, K. R. 1975 Wall mass transfer in laminar pulsatile flow in a tube. *A.I.Ch.E. J.* **21**, 259.

POPOV, D. A. 1975 Problems with discontinuous boundary conditions and the diffusion boundary-layer approximation. *Prikl. Mat. Mekh.* **39**, 93 (English trans.).

PROUDMAN, I. & PEARSON, J. R. A. 1957 Expansions at small Reynolds numbers for the flow past a sphere and a circular cylinder. *J. Fluid Mech.* **2**, 237.

SPRINGER, S. G. 1974 The solution of heat transfer problems by the Wiener–Hopf technique. II. Trailing edge of a hot film. *Proc. Roy. Soc.* A **337**, 395.

SPRINGER, S. G. & PEDLEY, T. J. 1973 The solution of heat transfer problems by the Wiener–Hopf technique. I. Leading edge of a hot film. *Proc. Roy. Soc.* A **333**, 347.